

System optimization of a long-range Brillouin-loss-based distributed fiber sensor

Yongkang Dong,^{1,2} Liang Chen,¹ and Xiaoyi Bao^{1,*}

¹Fiber Optics Group, Department of Physics, University of Ottawa, Ottawa, Canada, K1N 6N5

²e-mail: aldendong@gmail.com

*Corresponding author: xbao@uottawa.ca

Received 12 May 2010; revised 16 August 2010; accepted 19 August 2010;
posted 24 August 2010 (Doc. ID 128332); published 10 September 2010

We report a high-performance 25 km Brillouin-loss-based distributed fiber sensor through optimizing system parameters. First, the Brillouin spectrum distortion and measurement error induced by the excess amplification on probe pulse are investigated, and the results indicate that a low continuous-wave pump power is essential to decrease the measurement error. Then an optimal pulse pair is determined through the differential Brillouin gain evolution along the entire sensing fiber in a differential pulse-width pair Brillouin optical time domain analysis. Using dispersion-shifted fiber to allow a high-power probe pulse, we realize a 25 km sensing range with a spatial resolution of 30 cm and a strain accuracy of $\pm 20 \mu\epsilon$, which we believe is the best performance in such a length, to the best of our knowledge. © 2010 Optical Society of America

OCIS codes: 280.4788, 290.5900.

1. Introduction

For two decades, distributed Brillouin optical fiber sensors have gained much interest for their potential capability of monitoring temperature and strain, which find applications in civil and structural engineering, environmental monitoring, and geotechnical engineering. Brillouin scattering can be enhanced by stimulated Brillouin scattering (SBS) in a Brillouin optical time domain analysis (BOTDA) [1–3], which has a more intense signal and better spatial resolution compared with a spontaneous scattering based Brillouin optical time domain reflectometry [4–6]. At present, there have been two schemes to realize a BOTDA, including Brillouin gain [1,2] and Brillouin loss [3]. In a Brillouin-gain-based sensor, the pulsed light is used as a pump and has a high frequency over the continuous-wave (CW) light, so that the CW light experiences gain through the SBS process; on the

contrary, in the case of Brillouin loss, the CW light used as a pump experiences loss after propagating the sensing fiber.

For a short-range fiber, without pump depletion in the Brillouin gain case and excess amplification on the probe pulse in the Brillouin loss case, these two methods can get the same results. However, in a long-range BOTDA using Brillouin gain, the maximum input power of the CW light is severely limited by the pump depletion to the pump pulsed light, which decreases the Brillouin signal and also induces measurement errors in the far end of the fiber. In addition, increasing the pump pulse power can aggravate the pump depletion effect [7]. Therefore, care must be taken when one increases the pump pulse and CW light power in a Brillouin-gain-based BOTDA. In a Brillouin-loss-based system, the excess amplification on probe pulse induced by the CW pump can also distort the Brillouin spectrum and produce measurement errors in the far end of the sensing fiber. However, increasing the probe pulse power will not aggravate the excess amplification

0003-6935/10/275020-06\$15.00/0

© 2010 Optical Society of America

effect, so that a high-power probe pulse can be used to improve the signal-to-noise ratio (SNR).

In this paper, we first investigated the impact on the Brillouin spectrum induced by excess amplification on the probe pulse through changing the CW pump power, and the results indicate that a low CW pump power is essential to decrease the measurement error. A dispersion-shifted fiber with normal dispersion was used to allow a high-power probe pulse to improve the SNR without modulation instability (MI). Then we showed that the Brillouin gain saturation can cause a differential Brillouin gain decrease, and, thus, a specific pulse pair should be chosen to obtain the maximum differential gain in a differential pulse-width pair BOTDA. In addition, an optimal pulse pair was also considered to balance the differential gain along the entire 25 km sensing fiber.

2. Experimental Setup

The experimental setup is shown in Fig. 1. Two narrow linewidth (3 kHz) fiber lasers operating at 1550 nm are used to provide the probe and pump light, respectively, whose frequency difference is locked by a phase locking loop in a frequency counter and is automatically swept by varying the temperature of the fiber Bragg grating (FBG) of the cavity controlled by a computer. A 12 GHz bandwidth high-speed detector is used to measure the beat signal between the probe and pump, which provides feedback to the frequency counter to lock the frequency. The probe laser is launched to a high extinction ratio electro-optic modulator (EOM) to create a probe pulse with an extinction ratio higher than 45 dB. Before being launched into the sensing fiber, the probe pulse is amplified by an erbium-doped fiber amplifier (EDFA). A polarization scrambler is used to change the polarization state of the probe pulse continuously to reduce the polarization-mismatching-induced fluctuation on the signal by averaging a large number of signals. A FBG with a 3 dB bandwidth of 0.03 nm was used in front of the detector to filter out this

Rayleigh scattering noise of the probe pulse. Then a high-performance Brillouin distributed sensor is demonstrated in a 25 km dispersion-shifted fiber with the differential pulse technique and optimal parameters.

3. Excess Amplification on Probe Pulse in Long-Range Fibers

The pump depletion for the Brillouin-gain-based sensor and the excess amplification on the probe pulse for the Brillouin loss case are the major limiting factors for long-range sensing [8,9]. We studied the excess amplification effect in the probe pulse for the Brillouin loss case in a 20 km SMF-28 fiber by heating a 20 m segment, and we measured the Brillouin loss spectra via switching the pump and probe waves, as shown in Fig. 2. For case 1, the 20 m heated segment is in the far end of the sensing fiber in terms of probe pulse; while for case 2, through switching the pump and probe waves, the heated segment becomes the near end.

The Brillouin loss spectra were measured by using a 20 ns probe pulse with a peak power of 200 mW. Figure 3 shows the measured Brillouin spectrum width as a function of distance with a pump power of 1 mW, where all the sensing fiber was placed at room temperature with an average Brillouin frequency shift (BFS) of 10,867 MHz. As the distance increases, the Brillouin spectrum width decreases from 38.3 MHz to 28.7 MHz with a slope of ~ -0.5 MHz/km. This spectral width decreasing is caused by the probe pulse amplification from the pump wave at around the average BFS, which causes the probe pulse power to be unequal at the far end of the sensing fiber at a different frequency offset between pump and probe waves. It seems that the narrow spectra in the far end of the sensing fiber could improve the measurement accuracy. However, a considerable error could be induced when the fiber in the far end has a frequency shift with respect to the average BFS.

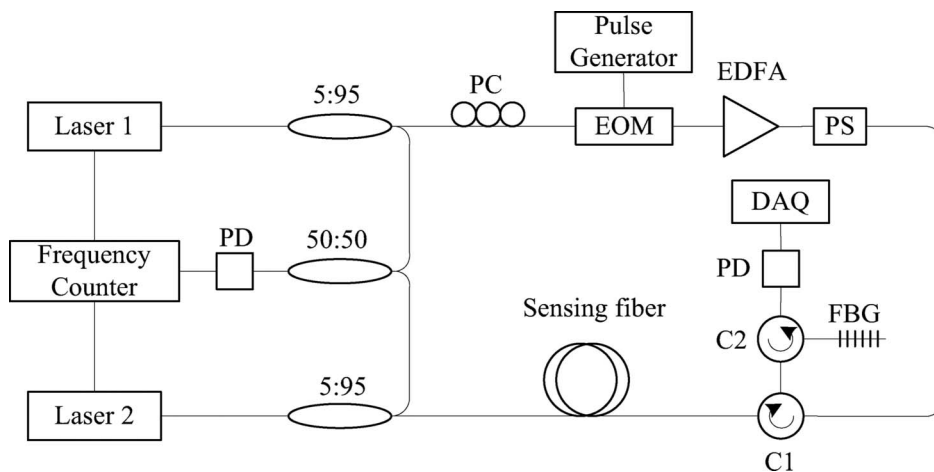


Fig. 1. Experimental setup: PD, photodetector; PC, polarization controller; PS, polarization scrambler; C, circulator; and DAQ, data acquisition.

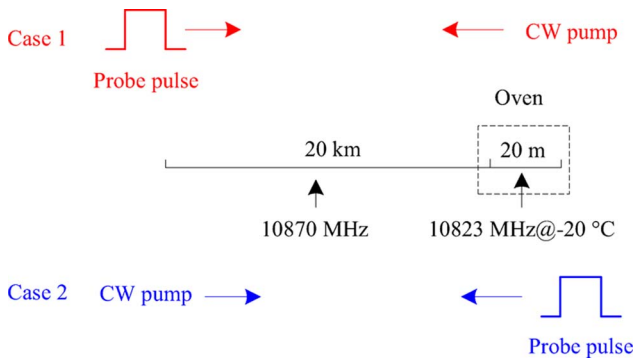


Fig. 2. (Color online) Sensing fiber and relative position of the pump and probe waves.

The temperature of the oven was controlled at $-20\text{ }^{\circ}\text{C}$, and the BFS of the fiber in the oven was 10,823 MHz, which has a difference of 44 MHz with respect to the average BFS. The Brillouin loss spectra were measured in both cases, as shown in Fig. 2, with different CW pump powers of 1, 0.6, 0.3, and 0.1 mW, and the results are shown in Fig. 4. In case 1 with the 1 mW CW pump, the measured spectrum shows distortion with the bump around the average BFS, as shown in Fig. 4(a). This is because when the frequency offset between the pump and probe is scanned to the average BFS, the probe pulse get excess amplification

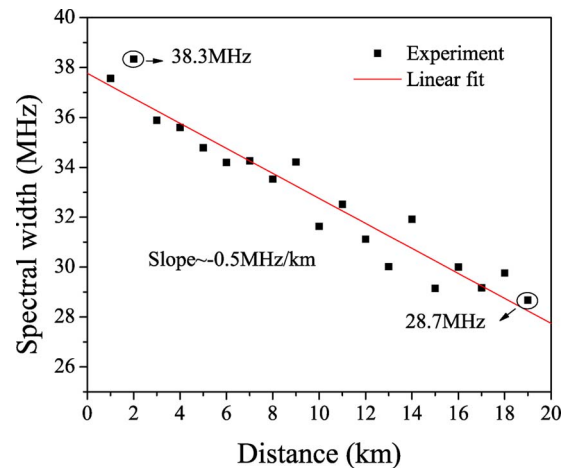


Fig. 3. (Color online) Measured Brillouin spectrum width as a function of distance with a CW pump power of 1 mW.

and can get more energy from the CW pump wave in the far end of the fiber, and thus induces a strong Brillouin loss signal around the average BFS, which inevitably distorts the spectrum. After switching the pump and probe waves in case 2, the measured spectrum shows a good Lorentzian profile because of no excess amplification on the probe pulse. As the CW pump power reduces, this bump around the average BFS on the spectrum weakens, and two spectra

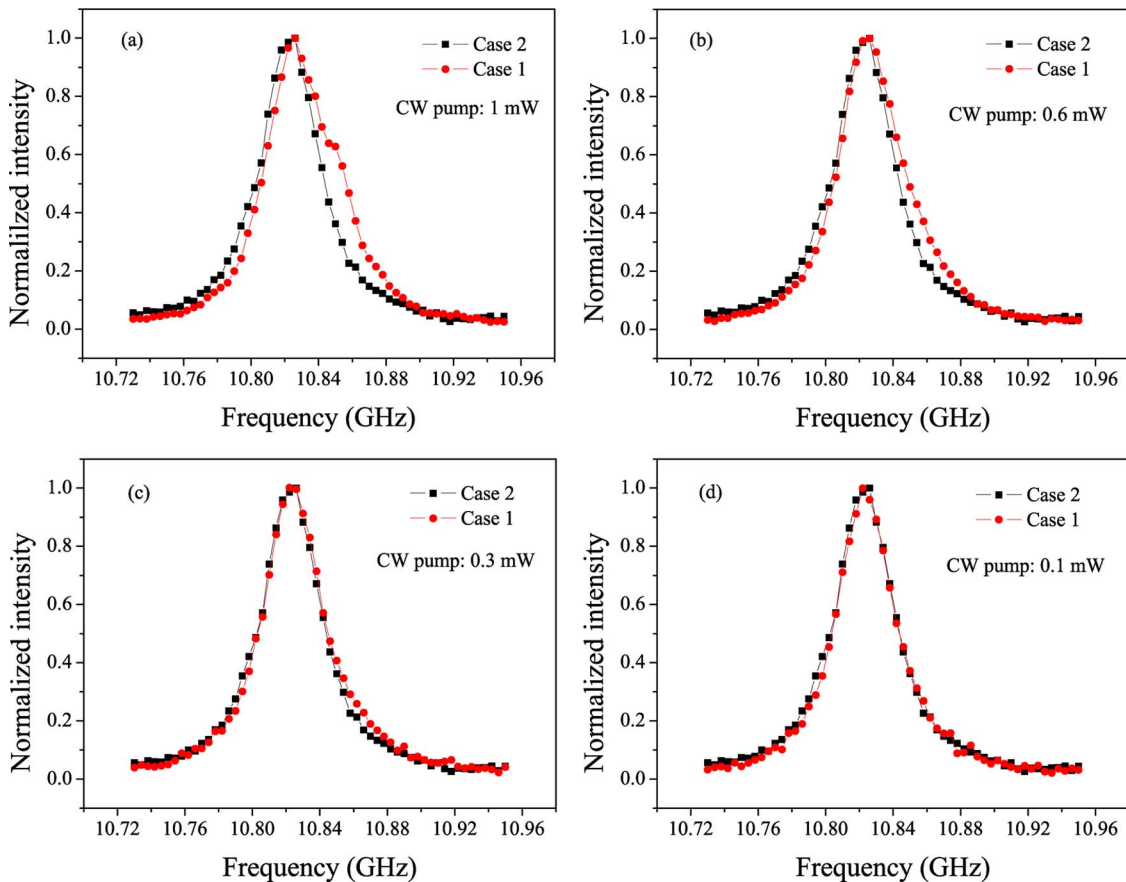


Fig. 4. (Color online) Measured Brillouin loss spectra for case 1 and case 2 at different CW pump powers: (a) 1, (b) 0.6, (c) 0.3, and (d) 0.1 mW.

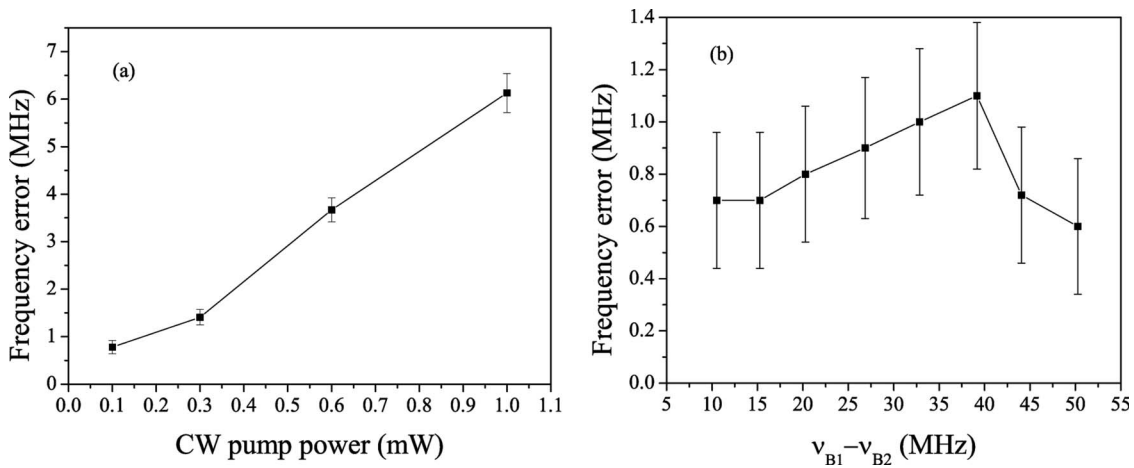


Fig. 5. Frequency error induced by the probe pulse amplification in the far end of 20 km sensing fiber at: (a) different CW pump power with a BFS difference of 44 MHz and (b) different BFS difference with a CW pump power of 0.1 mW.

measured in two cases tend to be the same. Figure 5(a) gives the fitting frequency error induced by the probe pulse amplification at different CW pump power. This frequency error is as high as 6 MHz for the 1 mW pump and only 0.7 MHz for the 0.1 mW pump, which shows that the CW pump power should be kept low enough to reduce the measurement error.

Then we investigated the frequency error induced by the probe pulse amplification at a different BFS difference between the heated far-end fiber and normal-condition fiber through changing the oven temperature. The CW pump power was set at 0.1 mW, the BFS difference was changed from 10 MHz to 50 MHz, and the results are shown in Fig. 5(b). It can be seen that a maximum frequency error is found at 40 MHz, beyond which it sharply decreases. It is easy to understand that the excess amplification on the probe pulse pulls the Brillouin spectrum from the actual one to the normal-condition BFS at the far-end fiber, so that at first the measured frequency error may increase with increasing the BFS difference between the far-end fiber and normal-condition fiber, then as the BFS difference increases beyond the Brillouin gain bandwidth, the impact of the excess amplification weakens, resulting in the

measured frequency error having a maximum value around the Brillouin gain bandwidth for a specific pump power.

4. Differential Brillouin Gain Evolution

Recently, we proposed a differential pulse-width pair Brillouin optical time domain analysis (DPP-BOTDA) for high spatial resolution sensing [10,11]. In this scheme, a narrowband Brillouin spectrum and strong differential Brillouin gain signal can be obtained from the long pulse pair; while a high spatial resolution can be achieved by using a small pulse-width difference. However, the differential Brillouin gain signal has a decrease in SNR with respect to the direct Brillouin gain signals, which is a limitation to further improving the spatial resolution by reducing the pulse-width difference. In order to obtain high spatial resolution with small pulse-width difference in a long-range fiber, it is essential to improve the SNR of direct Brillouin gain signals by increasing the probe pulse power, which, however, is limited by the MI effect in a long standard single-mode fiber [12,13]. The MI effect is a result of the interplay between the self-phase modulation (Kerr effect) and anomalous dispersion [14]. To avoid the MI effect in a BOTDA system and

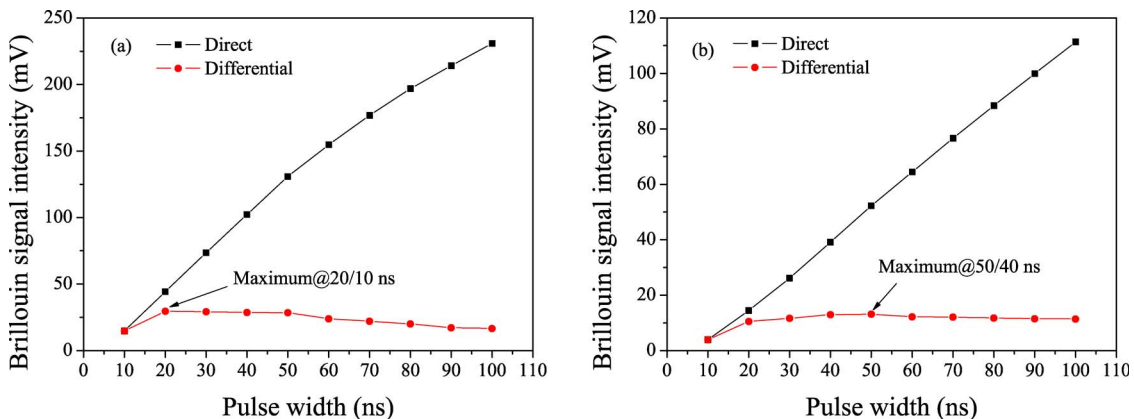


Fig. 6. (Color online) Direct and differential Brillouin signal intensities for different pulses (10 – 100 ns) at positions of (a) 1 and (b) 24 km, respectively; here, for the differential Brillouin signal, the pulse width refers to the longer pulse of the pulse pair.

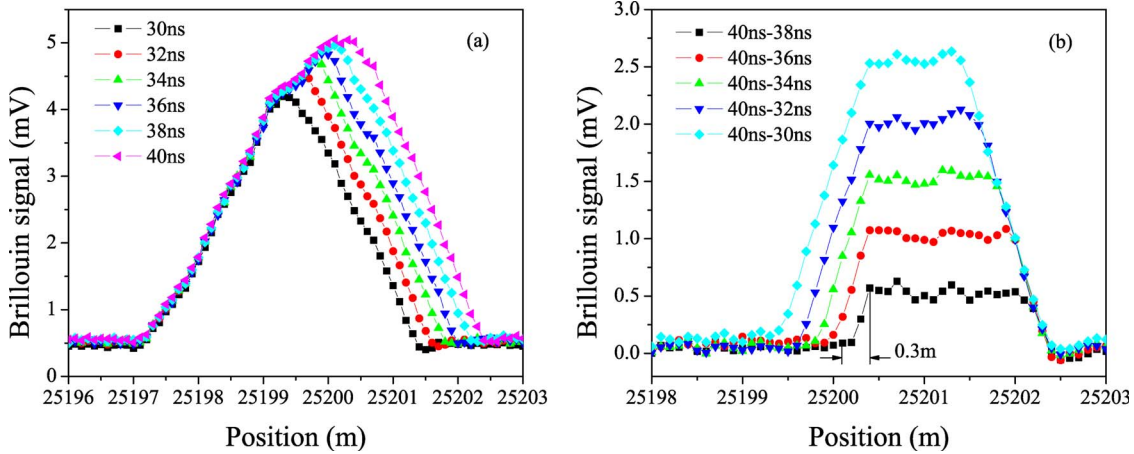


Fig. 7. (Color online) (a) Direct and (b) differential Brillouin signals for different pulses (30 – 40 ns) and pulse pairs (40/38 – 40/30 ns), respectively.

thus improve the SNR and spatial resolution in a long-range sensing fiber using a high-power probe pulse, we use a 25 km dispersion shifted fiber with normal dispersion at $\sim 1.5 \mu\text{m}$, which has a dispersion parameter of $\sim -1.4 \text{ ps/km}\cdot\text{nm}$ (compared with $\sim +17 \text{ ps/km}\cdot\text{nm}$ for SMF-28 fiber) and a BFS of 10,520 MHz at room temperature.

In the DPP-BOTDA scheme, although the spatial resolution is determined by the pulse-width difference and long pulses are preferable to get narrow Brillouin spectrum, the Brillouin gain could be saturated with long pulses, which decreases the differential Brillouin gain and consequently deteriorates the SNR and frequency accuracy. To find an optimal pulse pair and get a uniform differential Brillouin gain over the entire sensing length, we first investigate the evolution of the differential Brillouin gain at the beginning and ending of the fiber. The frequency offset is fixed at 10,520 MHz, and the probe pulse and pump power are 400 mW and 0.1 mW, respectively.

Figure 6 shows the direct and differential Brillouin signal intensities as a function of pulse width (10–100 ns with a step of 10 ns) at positions of 1 km (beginning fiber) and 24 km (ending fiber), where for the differential Brillouin signal, the pulse pairs are from 10/0 to 100/90 ns with a 10 ns pulse-width difference. As the probe pulse-width increases, the CW pump depletion makes the direct Brillouin gain tend to be saturated, which makes the maximum differential gain occur at 20/10 ns pulse pair at the position of 1 km, as shown in Fig. 6(a). However, for the position of 24 km, the probe pulse power is decreased due to the fiber attenuation, so that the CW pump depletion and direct gain saturation are postponed to the longer pulse width, and, consequently, the maximum differential gain occurs at 50/40 ns, as shown in Fig. 6(b). Considering the relatively small Brillouin loss signal in the far end of the sensing fiber, to balance the differential gain along the entire sensing fiber, we use a 40 ns pulse as the longer one in the pulse pair in the following DPP-BOTDA experiment.

In the experiment, a 2 m segment in the far end of the 25 km sensing fiber was stressed, which had a BFS of 10,630 MHz. All the time traces of the Brillouin signal were obtained by 2000 times average. Fixing the frequency offset at 10,630 MHz, Brillouin signals of the 2 m stressed fiber with different probe width from 30 ns to 40 ns with a step of 2 ns are plotted in Fig. 7(a), respectively. Figure 7(b) shows the differential signals with pulse-width differences of 2, 4, 6, 8, and 10 ns with pulse pairs of 40/38, 40/36, 40/34, 40/32, and 40/30 ns, respectively. For differential gain signals, the effective probe pulse is the differential pulse, for example, 2 ns for the 40/38 ns pulse pair, and the start time is the trailing edge of the 38 ns pulse. That is why the position shift is different for individual pulse pairs shown in Fig. 7(b). This position shift is a constant along the sensing fiber for a specific pulse pair, so that the position can be corrected by subtracting this constant value.

As the pulse-width difference decreases, the spatial resolution is improved while the signal intensity decreases, as shown in Fig. 8, which is the limitation of further improving the spatial resolution. Theore-

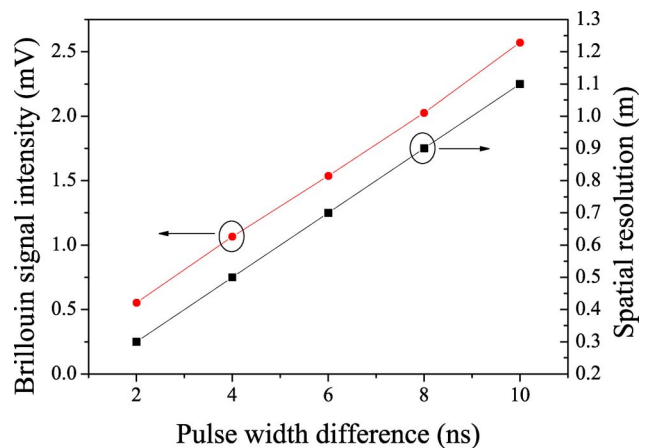


Fig. 8. (Color online) Brillouin signal intensity and spatial resolution for different pulse pairs in Fig. 7(b).

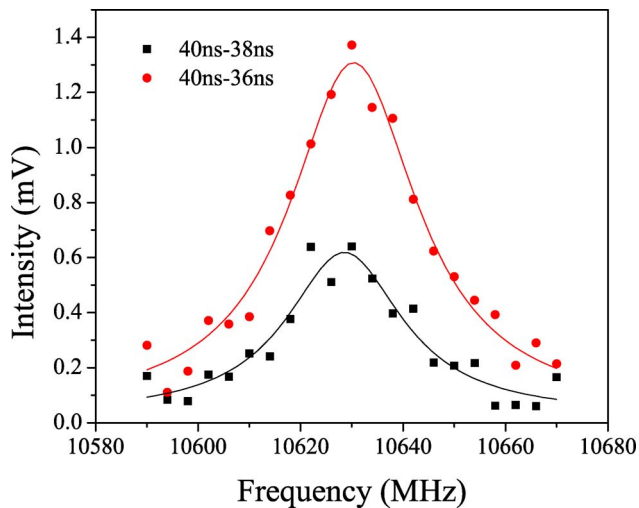


Fig. 9. (Color online) Measured Brillouin loss spectra of the stressed segment with 40/38 and 40/36 ns pulse pairs, respectively.

tically, the spatial resolution for DPP-BOTDA is only determined by the pulse-width difference. However, limited by the bandwidth of the detector, the final spatial resolution is actually determined by the differential pulse convoluting the response time of the detector. In our case, for example, the spatial resolution are 30 and 50 cm for 40/38 and 40/36 ns pulse pairs, respectively.

The measured Brillouin loss spectra of the stressed section using 40/38 and 40/36 ns pulse pairs are plotted in Fig. 9, respectively, which both exhibit a Brillouin spectrum width of ~ 30 MHz. The uncertainty of the central frequency of Lorentzian fitting are $\sim \pm 1$ and ± 0.5 MHz for 40/38 and 40/36 ns pulse pairs, which correspond to strain accuracy of ± 20 and $\pm 10 \mu\epsilon$, respectively.

5. Discussion and Conclusions

For a Brillouin-loss-based distributed fiber sensor, the probe pulse will get gain and be amplified after interaction with the CW pump wave. However, in a long-range sensing fiber, a CW pump wave may produce excess amplification on the probe pulse and cause a distorted Brillouin spectrum in the far end of the fiber, which may induce measurement errors. The measurement error induced by the excess amplification on the probe pulse is manifested when the BFS difference between the far-end fiber and normal-condition fiber is around the Brillouin gain bandwidth. This suggests that a low-power CW pump wave is preferable to avoid Brillouin spectrum distortion and measurement error in the far end of the fiber in a long-range sensing.

The direct Brillouin gain saturation induced by the CW pump wave depletion decreases the differential Brillouin gain, so that there is an optimal pulse pair to get the maximum differential Brillouin signal. In our experiment, we used a 40 ns pulse as the long pulse in the pulse pair to balance the differential

gain along the entire sensing fiber. Based on the analysis, we chose a 0.1 mW pump wave and a 400 mW probe pulse in a 25 km dispersion-shifted fiber for a Brillouin-loss-based fiber sensor. 40/38 and 40/36 ns pulse pairs were used to implement differential pulse measurement, and a spatial resolution of 30 and 50 cm with a strain accuracy of ± 20 and $\pm 10 \mu\epsilon$ were realized, respectively.

This work is supported by the Natural Sciences and Engineering Research Council of Canada (NSERC) via the Discovery Grant and Canada Research Chair Program.

References

1. X. Bao, D. J. Webb, and D. A. Jackson, "22 km distributed temperature sensor using Brillouin gain in an optical fiber," *Opt. Lett.* **18**, 552–554 (1993).
2. M. Nikles, L. Thevenaz, and P. A. Robert, "Simple distributed fiber sensor based on Brillouin gain spectrum analysis," *Opt. Lett.* **21**, 758–760 (1996).
3. X. Bao, D. J. Webb, and D. A. Jackson, "32 km distributed temperature sensor based on Brillouin loss in an optical fiber," *Opt. Lett.* **18**, 1561–1563 (1993).
4. K. Shimizu, T. Horiguchi, Y. Koyamada, and T. Kurashima, "Coherent self-heterodyne detection of spontaneously Brillouin-scattered light waves in a single-mode fiber," *Opt. Lett.* **18**, 185–187 (1993).
5. T. R. Parker, M. Farhadiroushan, V. A. Handerek, and A. J. Rogers, "Temperature and strain dependence of the power level and frequency of spontaneous Brillouin scattering in optical fibers," *Opt. Lett.* **22**, 787–789 (1997).
6. S. M. Maughan, H. H. Kee, and T. P. Newson, "57 km single-ended spontaneous Brillouin-based distributed fiber temperature sensor using microwave coherent detection," *Opt. Lett.* **26**, 331–333 (2001).
7. T. Horiguchi, K. Shimizu, T. Kurashima, M. Tateda, and Y. Koyamada, "Development of a distributed sensing technique using Brillouin-scattering," *J. Lightwave Technol.* **13**, 1296–1302 (1995).
8. E. Geinitz, S. Jetschke, U. Ropke, S. Schroter, R. Willsch, and H. Bartelt, "The influence of pulse amplification on distributed fiber-optic Brillouin sensing and a method to compensate for systematic errors," *Meas. Sci. Technol.* **10**, 112–116 (1999).
9. A. Minardo, R. Bernini, L. Zeni, L. Thevenaz, and F. Briffod, "A reconstruction technique for long-range stimulated Brillouin scattering distributed fiber-optic sensors: experimental results," *Meas. Sci. Technol.* **16**, 900–908 (2005).
10. W. Li, X. Bao, Y. Li, and L. Chen, "Differential pulse-width pair BOTDA for high spatial resolution sensing," *Opt. Express* **16**, 21616–21625 (2008).
11. Y. Dong, X. Bao, and W. Li, "Differential Brillouin gain for improving the temperature accuracy and spatial resolution in a long-distance distributed fiber sensor," *Appl. Opt.* **48**, 4297–4301 (2009).
12. M. N. Alahbabi, Y. T. Cho, T. P. Newson, P. C. Wait, and A. H. Hartog, "Influence of modulation instability on distributed optical fiber sensors based on spontaneous Brillouin scattering," *J. Opt. Soc. Am. B* **21**, 1156–1160 (2004).
13. D. Alasia, M. G. Herraes, L. Abrardi, S. M. Lopez, and L. Thevenaz, "Detrimental effect of modulation instability on distributed optical fiber sensors using stimulated Brillouin scattering," *Proc. SPIE* **5855**, 587–590 (2005).
14. G. P. Agrawal, *Nonlinear Fiber Optics* (Academic, 1995).